J. Membrane Biol. 207, 107–117 (2005)
DOI: 10.1007/s00232-005-0805-0

The Journal of
Membrane
Biology

Slow Sodium Channel Inactivation and Use-dependent Block Modulated by the Same Domain IV S6 Residue

M. Carboni, Z.-S. Zhang, V. Nepliouevа, C.F. Starmer, A.O. Grant
Departments of Pediatrics and Medicine, Duke University Medical Center, Box 3504 Durham, NC 27710, USA, and Department of Biometry, Medical University of South Carolina, Durham, NC, USA

Received: 25 October 2004/Revised: 22 October 2005

Abstract. Voltage- and/or conformation-dependent association and dissociation of local anesthetic-class drugs from a putative receptor site in domain IV S6 of the sodium channel and slow conformation transitions of the drug-associated channel have been proposed as mechanisms of use- and frequency-dependent reduction in sodium current. To distinguish these possibilities, we have explored the reactivity to covalent modification by thiols and block of the mutations F1760C and F1760A at the putative receptor site of the cardiac sodium channel expressed as stable cell lines in HEK-293 cells. Both mutations decreased steady-state fast inactivation, shifting V1/2h from −86 ± 1.3 mV (WT) to −72.3 ± 1.4 mV (F1760C) and −67.7 ± 1 mV (F1760A). In the absence of drug, the F1760C mutant channel displayed use-dependent current reduction during pulse-train stimulation, and faster onset of slow inactivation. This mutant also retained some sensitivity to lidocaine. In contrast, the F1760A mutant showed no use-dependent current reduction or sensitivity to lidocaine. The covalent-modifying agent MTS-ET enhanced use-dependent current reduction of the F1760C mutant channel only. The use-dependent reduction in current of the covalently modified channel completely recovered with rest. Lidocaine produced no additional block during exposure to MTS-ET-treated cells (MTS-ET 43 ± 2.7%: MTS-ET lidocaine 47 ± 4.5%), implying interaction at a common binding site. The data suggest that use-dependent binding at the F1760 site results in enhanced slow inactivation rather than alteration of drug association and dissociation from that site and may be a general mechanism of action of sodium-channel blocking agents.

Correspondence to: A.O. Grant; email: grant007@mc.duke.edu

Key words: Cardiac sodium channel — Slow inactivation — Anti-arrhythmic drug action

Introduction

Local anesthetics and class I antiarrhythmic drugs suppress excitability by reducing the sodium current in a use-dependent manner (Strichartz, 1973; Bean, Shrager & Goldstein, 1981; Hondeghem & Katzung, 1977). Models of this action postulate that sodium channel states populated at depolarized potentials have a greater affinity for drugs than do resting channels. These states include the open state and multiple inactivated states. Usually, binding occurs during depolarization and is dissipated in the intervals between depolarizations. If the interval between depolarizations is less than the time required for complete drug dissociation, cumulative block occurs with repeated pulses (use-dependent block).

Block of open sodium channels can be readily demonstrated by a reduction of the mean open time of single sodium-channel current (Kohlhardt, Fichtner & Froebe, 1987; Grant et al., 1993) and by alterations of the time course of the whole-cell sodium current. The demonstration of block of inactivated channel states requires the use of pulse protocols with pre-potentials that shift channels into the desired conformation for variable periods, followed by activating pulses. The reduction of block when fast inactivation is reduced chemically or with site-directed mutagenesis suggests that it plays a central role in the blocking process (Matsuki et al., 1984; Zaborovskaya & Khodorov, 1984; Grant et al., 2000). However, recent studies using the cysteine accessibility method show that fast inactivation recovers normally in Na_v 1.4 sodium channels ex-

posed to lidocaine (Vedantham & Cannon, 1999). This suggests distinct pathways for recovery from block and inactivation. Sodium channels enter multiple inactivated states during sustained depolarization. Slow or intermediate inactivation has also been proposed as putative states for block. Much less is known about these states compared with the fast inactivated state (Kambouris et al., 1998).

These observations must be reconciled with the striking reduction in sodium channel sensitivity to local anesthetic-class drugs produced by the F1764A mutation in the inner pore region of the sixth transmembrane segment of domain IV of rNa_v 1.2 sodium channels (Ragsdale et al., 1994). This mutation shifts the voltage dependence of fast inactivation to more depolarized potentials. However, its effect on slow inactivation has not been described. We examined whether the nature of F1760 (equivalent to F1764 in the rat brain sequence) substituents would influence slow inactivation and use-dependent current reduction in the human cardiac sodium channel, hNa_v 1.5.

The F1760C mutation in Na_v 1.5 permitted the covalent modification of the receptor site with methanethiosulfonate ligands of varying size and charge, e.g., [2−(trimethylammonium)ethyl] methanethiosulfonate (MTS-ET) and (2-sulfonate ethyl)methanethiosulfonate (MTS-ES). A change in the kinetics of slow inactivation with different substituents would provide a mechanistic link between the critical role of F1760 mutants and changes in slow inactivation documented by mutations at other sites. If the [2-(trimethylammonium)ethyl] adduct of MTSET (or that of MTS-ES) is covalently anchored to the receptor, rest recovery cannot be explained by dissociation of the adduct. Further, if the reaction is covalent, additional block by lidocaine acting at the same site should be minimal.

Materials and Methods

Construction of Stable Cell Lines Containing DIV, S6 Mutations

The mutations F1760A, F1760C, and W374A/F1769C were performed by overlap PCR. Stable transfectants were established in HEK-293 cells using dominant selective markers.

Experimental Set-up

Whole-cell sodium channel currents were recorded from cells expressing the wild-type and mutant sodium channels. Cells were superfused with external solution containing (mM): NaCl 130, KC1 4, $CaCl_2$ 1, $MgCl_2$ 5, HEPES 5, glucose 5 (pH 7.4 with NaOH). Micropipettes were filled with cesium internal solution containing (mM): CsCl 130, $MgCl_2$ 1, Mg ATP 5, Cs-EGTA 10, HEPES 10 (pH 7.2 with CsOH). The cesium ions blocked the endogenous potassium currents present in these cells (Zhu et al., 1998). Under these recording conditions, the sodium current was the only measurable ionic current. All experiments were performed at room temperature (20–22°C).

Voltage-clamp protocols were performed in four different conditions: baseline, external exposure to 800 μM of lidocaine, internal exposure to 3 mM MTS-ET (Toronto Research Chemicals, North York, Ontario), and exposure to both external lidocaine and internal MTS-ET. In preliminary experiments, external application of MTS-ET and both internal and external application of MTS-ES were without effect. A lidocaine concentration of 800 μM was chosen because the F1760C mutant has markedly reduced lidocaine sensitivity. The lowest lidocaine concentration that produced definitive effects in experiments involving the F1760C mutant was 800 μM. MTS-ET solution was prepared fresh from powder and dissolved in the cesium pipette solution. MTS-ET solution was discarded and remade fresh following one hour of use.

Recording Techniques

Whole-cell currents were recorded with 0.5–1.0 MΩ microelectrodes using a Dagan 3900A integrating patch-clamp amplifier (Dagan, Minneapolis, MN). A silver/silver chloride wire coupled each microelectrode to the input of the amplifier. A similar wire embedded in an agar/micropipette solution formed the bath reference. Series resistance compensation used conventional and supercharging techniques. At the beginning of each whole-cell experiment, adequacy of voltage control was assessed as previously described (Gilliam, Starmer & Grant, 1989). The holding potential for all experiments was maintained at −100 mV unless otherwise stated. The current-voltage relationship was determined with 40 ms pulses of increasing amplitude applied at 1400 ms intervals. The pulse amplitude was incremented in 5 mV steps from a potential of −80 mV to +30 mV. The steady-state fast inactivation curve was determined by the application of 500 ms prepulses from −130 to −15 mV. A 20 ms test pulse to −20 mV followed each prepulse. The prepulse potential was incremented in 5 mV steps. Whole-cell currents were filtered at 10 kHz and digitized at 40 kHz. Additional voltage-clamp protocols used are described within the results below.

Data Analysis

The analysis of whole-cell currents has been described in prior studies from this laboratory (Gilliam et al., 1989). Peak currents were measured with custom software written in C programming language. Inactivation curves were fit with Boltzmann functions:

$$h_\infty = 1/\left(1 + \exp\left[V - V_{1/2}\right]K_h\right) \quad (1)$$

using a Marquardt routine where h_∞ is the inactivation variable; V is the membrane potential, $V_{1/2}$ the potential at which $h = 0.5$ and k_h the slope factor. The activation voltage was derived from fitting the current-voltage curve using:

$$m_\infty = g_{max}(V - V_{rev})m^3/\left(1 - \exp\left[V - V_{1/2}\right]\right)/k_m \quad (2)$$

where g_{max}, $V_{1/2}$ and k_m were estimated using least squares; V_{rev} was estimated by extrapolation of the rising (positive) limb of the I-V curve. The time constant, τ, for the development of inactivation was obtained by fitting the following equation:

$$I(t) = I_0\exp(t/\tau) \quad (3)$$

where I_t is the test pulse current at prepulse duration t and I_0 the current at −20 mV in the absence of the inactivating prepulse. Test pulse current was normalized to the maximum prepulse current. Data are quoted as mean ± SEM. Comparisons of data obtained from the same cell were made with a paired t-test. Other comparisons were made with an unpaired t-test or analysis of variance; $P < 0.05$ was considered significant.

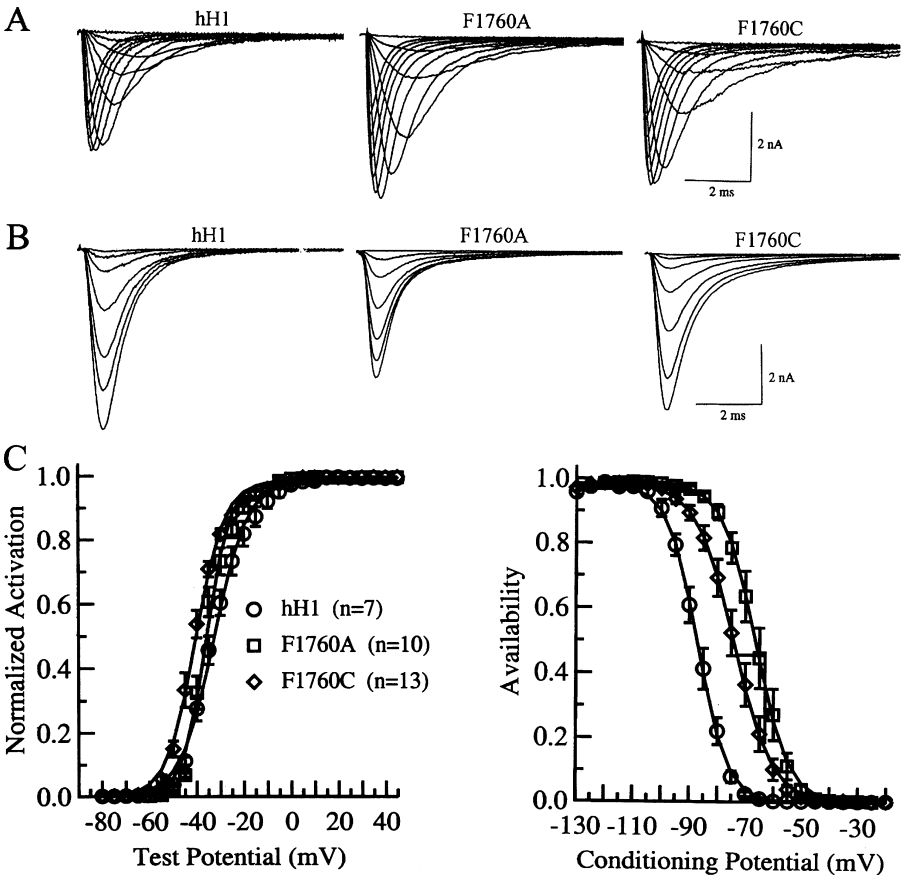

Fig. 1. Gating kinetics of wild-type (hH1), F1760A and F1760 cardiac sodium channels. (*A*) Membrane currents elicited by voltage pulses from a holding potential of −100 mV. The test potential was incremented from −80 to +30 mV in 5 mV steps. (*B*) Membrane currents elicited by test voltage steps at −20 mV following 500 ms conditioning pulses from −130 to −15 mV; the currents in the illustration were obtained at conditioning potentials of −100, −95, −90, −85, −80, −75 and −70 mV. The conditioning voltage was incremented in 5 mV steps. (*C*) Activation and inactivation curves of averaged data fitted to Boltzmann functions. Parameters of fits to the averaged data are summarized in Table 1.

Results

Gating Characteristics in the Absence of Drug

Non-transfected cells demonstrated no appreciable endogenous sodium current, whereas cells transfected with wild-type and the F1760C and F1760A mutant channels demonstrated robust sodium currents in the nano-ampere range. Cells expressing the double mutant W374A/F1760C displayed smaller currents that were less than one nA. Current-voltage relationships and steady-state fast inactivation (Fig. 1) were first determined for hH1, F1760A, and F1760C channels under baseline conditions. Gating parameters are summarized in Table 1. Compared to wild-type (WT), $V_{1/2m}$ of F1760A (FA) channels was ~5 mV more negative ($P < 0.05$) and the slope factor (k_m) smaller ($P < 0.05$). $V_{1/2m}$ of the F1760C (FC) mutant was shifted ~10 mV in the negative direction ($P < 0.05$) with no significant difference in k_m from that of WT or FA channels. The potential for half-inactivation ($V_{1/2h}$) of the FA mutant was shifted ~20 mV in the positive direction ($P < 0.05$) with no difference in k_h. $V_{1/2h}$ of FC channels were also shifted in a more positive direction from WT, but not to the degree of the FA mutant, ~14 mV ($P < 0.0001$ vs WT, $P < 0.05$ vs FA). The slope factor k_h was unchanged. From Fig. 1*B*, it is evident from the test currents obtained at −20 mV that the relaxation of the current for the FC mutant was slower than that of the wild type. The relaxation of the current in both cell types was well fit by single exponentials. The currents in Fig. 2*A* and *B* were obtained at the test potential −30 mV in the wild-type and FC mutant channels, respectively. The relaxation time constants were 0.95 and 2.8 ms. Summary data are presented in Fig. 2*C*. At potentials negative −20 mV, relaxation of the current was slower in the FC mutant. Peak currents of all three cell lines at baseline were similar.

Pulse Train Stimulation

Following determination of gating characteristics, we assessed the response of WT, FA, and FC channels to pulse train stimulation. Preliminary screening had shown that repetitive depolarization of the FC mutant resulted in use-dependent current reduction in the absence of drug, while WT and FA mutant channels demonstrated no significant use-dependent current reduction (1.5% and 0.9% for Hh1 and FA respectively). The use-dependent current reduction with the FC mutant was unexpected, since $V_{1/2h}$ for the FC channel was shifted in a more positive direction, indicating a greater Na-channel availability than

Table 1. Parameters of fast gating kinetics of wild-type and mutant channels

	hH1	F1760A	F1760C	F1760C/MTSET
Peak Current				
*I*P (nA)	−4.1 ± 1 (7)	−4.7 ± 0.5 (10)	−5.4 ± 0.5 (13)	2.3 ± 0.3 (11)
Activation				
$V_{1/2}$, mV (*n*)*	−32.0 ± 1.4 (7)	−36.4 ± 1.0 (10)	−42.4 ± 1.1 (13)	−57.5 ± 1.8 (11)
k_m	6.2 ± 0.5	−4.9 ± 0.2	5.4 ± 0.2	5.8 ± 0.2
Steady-State Fast Inactivation				
$V_{1/2}$, mV (*n*)**	−86.5 ± 1.3 (7)	−67.7 ± 1.0 (10)	−72.3 ± 1.4 (13)	−87.7 ± 2.1 (11)
k_h	4.8 ± 0.2	5.1 ± 0.1	5.3 ± 0.1	5.8 ± 0.4

*hH1 vs F1760 $p < 0.01$; F1760C vs F1760C/MTSET $p < 0.0001$
**hH1 vs F1760A $p < 0.001$; hH1 vs F1760C $p < 0.01$; F1760C vs F1760C/MTSET $p < 0.001$

WT at any given holding potential. From a holding potential of −90, −100 mV, and −120, forty 40 ms pulses were applied to a potential of −20 mV at cycle lengths (CL) of 150 to 2000 ms.

Neither WT nor FA mutant sodium channels exhibited use-dependent current reduction at any of the tested cycle lengths or holding potentials in the absence of drug. The FC mutant exhibited use-dependent current reduction that was both cycle length- and voltage-dependent (Fig. 3). The fractional reduction of current observed at a V_{hold} of −100 mV and cycle length 150 ms, 550 ms, and 1150 ms was 0.15 ± 0.01, 0.05 ± 0.005, and 0.01 ± 0.001, respectively. A substantially greater current reduction was observed at more depolarized holding potentials (V_{hold} −90 mV and CL 150 ms: 0.26 ± 0.04; CL 1500 ms: 0.01 ± 0.001). At more hyperpolarized holding potentials (e.g., V_{hold} −120 mV) no use-dependent current reduction was observed at any tested cycle length.

Because the FC mutant exhibited use-dependent current reduction in the absence of drug despite a positive shift in $V_{1/2h}$, other causes for reduced availability during repeated stimulation were entertained. One possible explanation accounting for the observed use-dependence is slowing in recovery from inactivation. Either recovery from fast inactivation is slowed in the FC mutant or the mutant channel enters a slow inactivated state with delayed recovery. We therefore tested each of these possibilities.

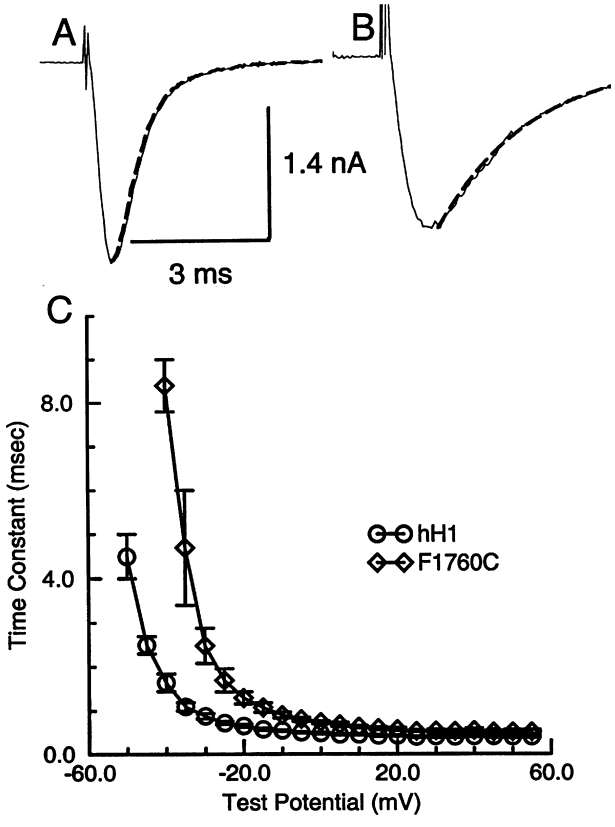

Fig. 2. Comparison of the current relaxation in the wild-type and FC mutant channel. *A* and *B* show current responses elicited from a holding potential of −100 mV to a test potential of −30 mV. The relaxation of the current was fit to a single exponential (broken line). Summary data are presented in *C*.

Recovery from Fast Inactivation

Recovery from inactivation for the WT and F/C mutant channel at a holding potential of −100 mV was measured using either a single conditioning pulse or a train of 20 pulses. The recovery interval was varied between 3 and 1300 ms. Summary data are illustrated in Fig. 4, and the time constants presented in Table 1. Using either conditioning-pulse format, the recovery process of the WT channel was fit to a single exponential with time constants that were not significantly different. For the F/C mutant channels, the recovery process was best fit by a bi-exponential. The time constants were similar for the single-pulse and the train conditioning protocols. However, the slow component of recovery was much larger with the pulse train conditioning protocol ($P < 0.05$), supporting an enhanced contribution of a slowly inactivating component.

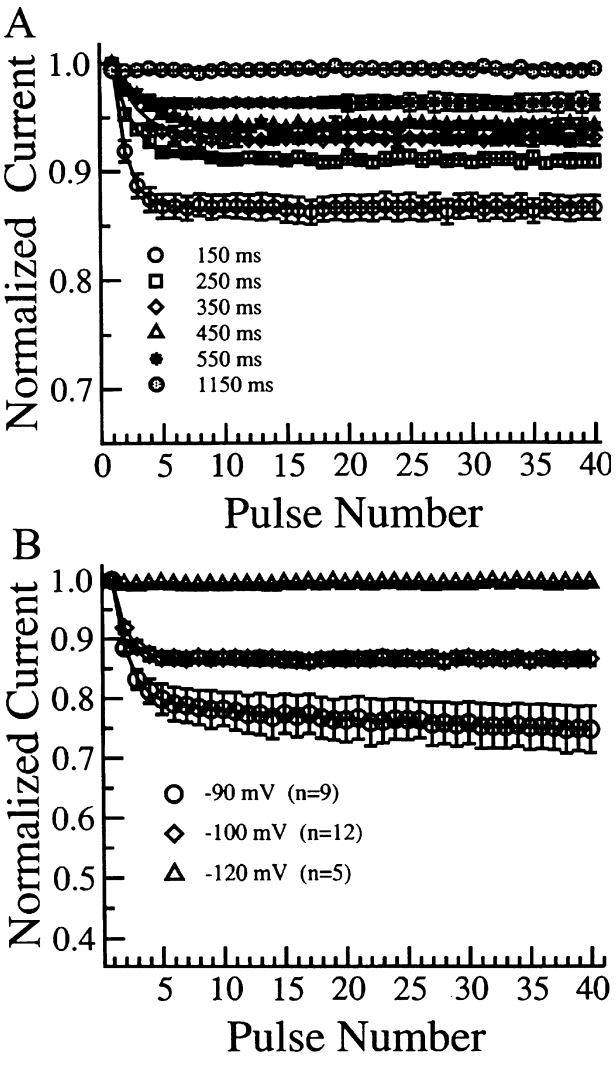

Fig. 3. Response of cells expressing the F1760C mutant sodium channels to pulse-train stimulation. (*A*) The holding potential was set at −100 mV and forty 40 ms pulses to −20 mV were applied at interpulse intervals of 150–1150 ms. Current during the n^{th} pulse was normalized to that of the first pulse of each train. (*B*) The interpulse interval was fixed at 150 ms, but the holding potential was varied from −120 to −90 mV.

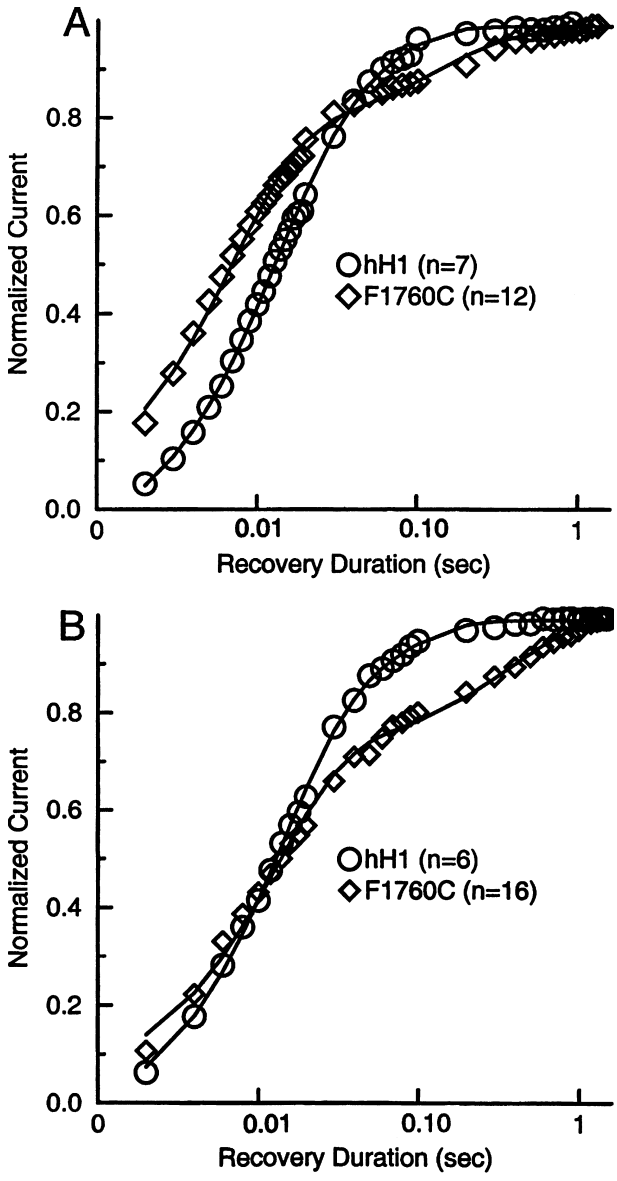

Fig. 4. Comparison of the kinetics of recovery from inactivation of wild-type (hH1) and F1760C mutant Na channels. (*A*) From a holding potential of −100 mV, a 40 ms inactivating pulse to −20 mV was applied. This resulted in inactivation of the current in cells expressing hH1 and the F1760C mutant. The conditioning pulse was followed after a variable recovery interval by a 20 ms test pulse to −20 mV. Test pulse currents were normalized to the conditioning pulse current, plotted against the recovery interval (logarithmic scale) and fit to one (hH1) or two (F1760C) exponentials. (*B*) Inactivation was effected by a train of twenty 40 ms pulses of interpulse interval 150 ms. Test pulses were similar to those used in Figure 3A.

Characteristics of Slow Inactivation

We used 10-second prepulses to induce slow inactivation and 10-second recovery intervals to allow recovery from slow inactivation. In order to assess the voltage-dependence of slow inactivation, cells were maintained at a holding potential of −100 mV. Ten-second prepulses were applied from −130 mV to +90 mV followed by a return to V_{hold} for 200 ms to allow recovery from fast inactivation. A 20 ms test pulse was then applied to −20 mV. V_{hold} was maintained for 10 seconds between each test pulse and the next prepulse to allow for recovery from slow inactivation. The prepulse potential was incremented in 5 mV steps. After 10 seconds at +90 mV, about half of both the WT and FC mutant channels entered a slow-inactivated state (Fig. 5*A*). Variability between cells was large. The slope factor for the FC channels was less than that of the wild-type channel, consistent with greater voltage dependence of slow inactivation of the FC channels.

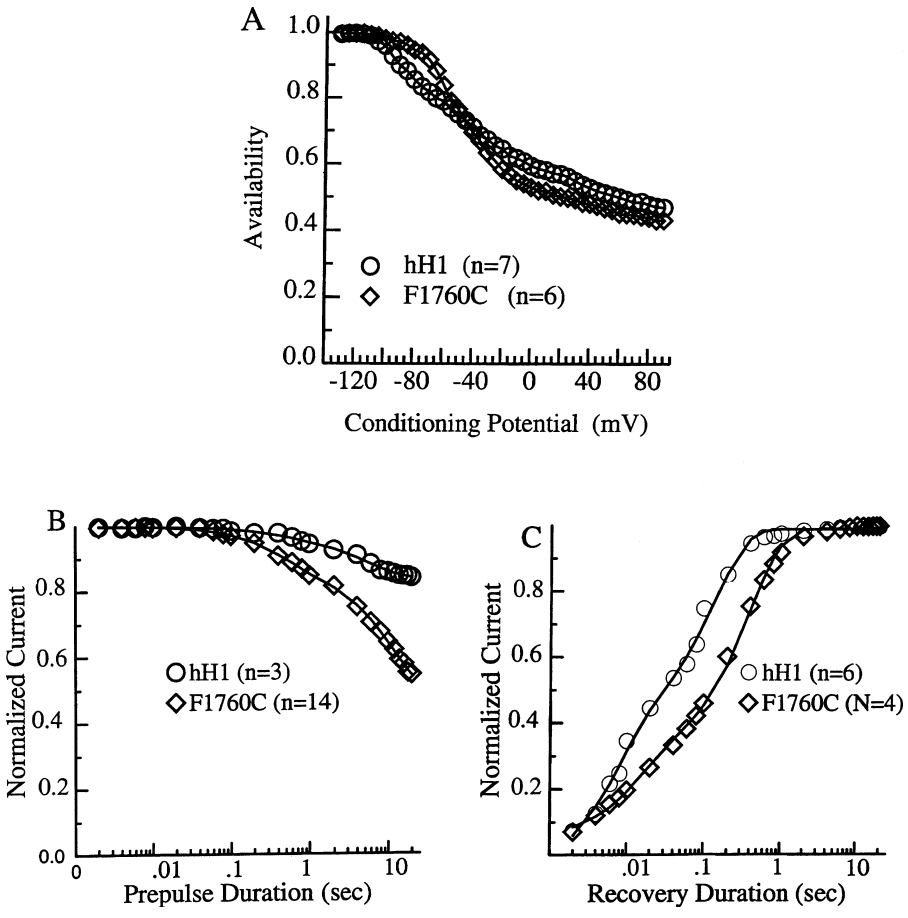

Fig. 5. Voltage-dependence kinetics of slow inactivation of the wild-type (hH1), and F1760C mutant sodium channels. (*A*) Voltage dependence of slow inactivation. Ten-second conditioning pulses were applied from −135 to +90 mV. After 200 ms recovery intervals, test pulses were applied to +60 mV. Normalized test pulse currents are plotted against conditioning voltage. (*B*) Kinetics of development of slow inactivation. From a holding potential of −100 mV, depolarizing pulses of variable duration were applied. The membrane potential was returned to −100 mV for 200 ms to permit recovery from fast inactivation. Test pulses to −20 mV were then applied. Normalized test-pulse current is plotted against the conditioning pulse duration (logarithmic scale). (*C*) Recovery from slow inactivation. 20 ms test pulses to −20 mV follow ten-second pulses to −20 mV after a variable recovery interval. Normalized test pulse current is plotted against the recovery interval (logarithmic scale).

Table 2. Parameters of recovery from inactivation

	hH1	F1760C	F1760C/MTSET
Recovery from fast inactivation			
τa, −100mV, ms (*n*)	17.9 ± 1.4 (7)	7.0 ± 1.0 (12)	12.4 ± 1.0 (6)
τb, −100mV, ms (*n*)		135.1 ± 10.0	147.1 ± 22.4
a; b		0.2 ± .01; 0.8 ± .01	
Recovery from use-dependent block			
τc, −100 mV, ms (*n*)	19.5 ± 3.2†‡ (6)	6.9 ± 0.7† (16)	12.8 ± 2.1‡ (11)
τd, −100 mV, ms (*n*)		370.0 ± 44.5	370.0 ± 72.0
c; d		0.3 ± .01; 0.7 ± .02	

†hH1 vs F1760 $p < 0.01$
‡hH1 vs F1760C/MTSET $p < 0.05$
n, the number of channels, is given in parentheses, a, b: fast and slow components of recovery from inactivation; c, d: fast and slow components of recovery from use-dependent block.

We determined whether kinetics differences in the rate of entry into or recovery from slow inactivation could account for the use-dependent current reduction in the FC channels. In order to assess the onset of slow inactivation, cells were maintained at a V_{hold} of −100 mV for 10 seconds. A prepulse of duration 2 ms to 20 s was then applied to +60 mV followed by return to V_{hold} for 200 ms to allow for recovery of fast inactivation. A 20 ms test pulse was then applied to a potential of −20 mV. Recovery from slow inactivation was determined by applying a 10-second prepulse to a potential of +60 mV from a V_{hold} of −100 mV. The cell was then clamped back to V_{hold} for 2 ms to 20 s followed by a 20 ms test pulse to −20 mV. Normalized currents were plotted and exponential fits obtained to determine the time constants for slow inactivation onset (Table 2, Fig. 5*B*) and recovery (Table 1, Figure 5*C*). The currents of WT and FC mutant channels were fit best with single exponential functions for both protocols. FC channels entered the slow inactivated state more rapidly at the depolarized conditioning potential and recovered

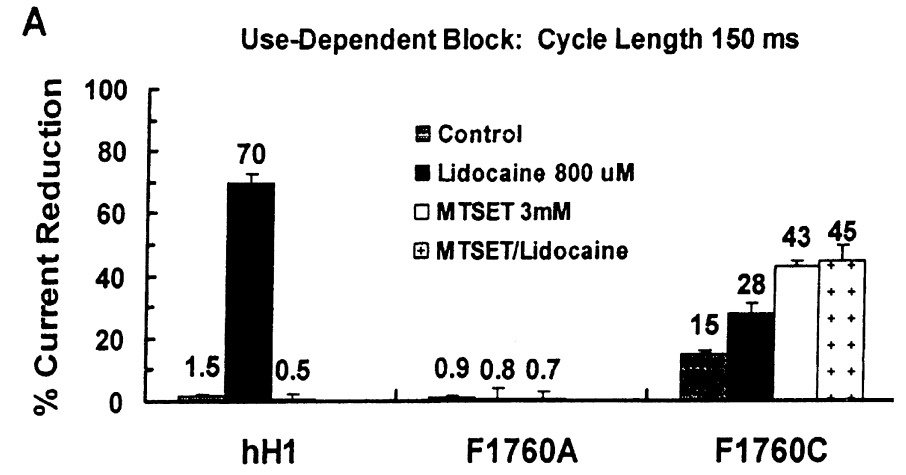

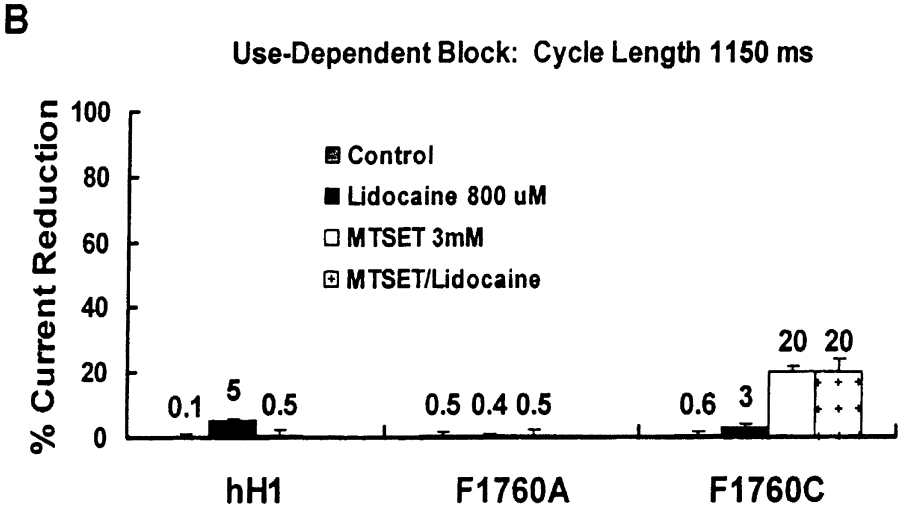

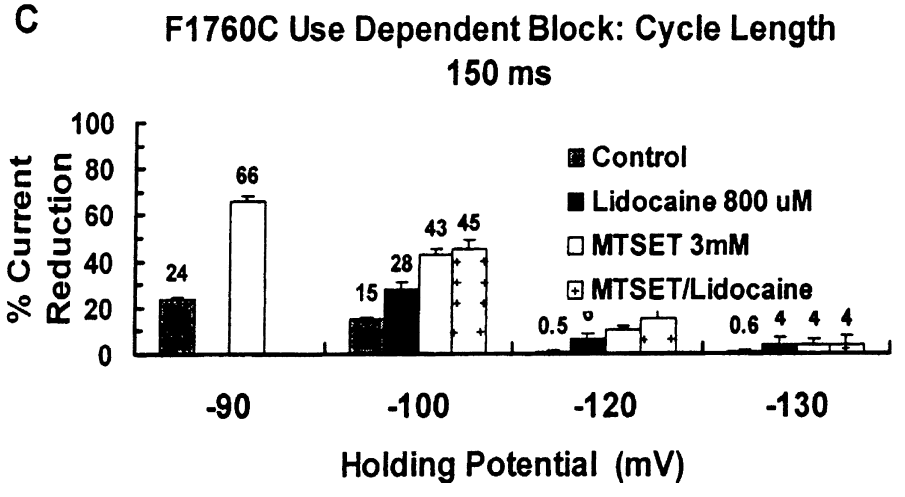

Fig. 6. Use-dependent block of wild-type, F1760A, and F1760C during control, exposure to 800 μM lidocaine, 3 mM MSET and lidocaine + MTSET. Cells were held at a membrane potential of −100 mV (panels *A* and *B*) and forty 40 ms pulses were applied to a test potential of −20 mV. The cycle length was 150 ms in panel *A* and 1150 ms in panel *B*. Results obtained with 150 ms pulse trains at holding potentials of −90, −100, −120 and −130 are illustrated in panel *C*.

more slowly at −100 mV than did WT channels ($P < 0.05$ for both). These kinetic differences in slow inactivation can account for the use-dependent current reduction in the FC mutant channels.

The W402A mutant in the rat skeletal sodium channel Na_v 1.4 attenuates slow inactivation and reduces channel blockade by lidocaine. To examine the effect of the analogous mutation on the use-dependent

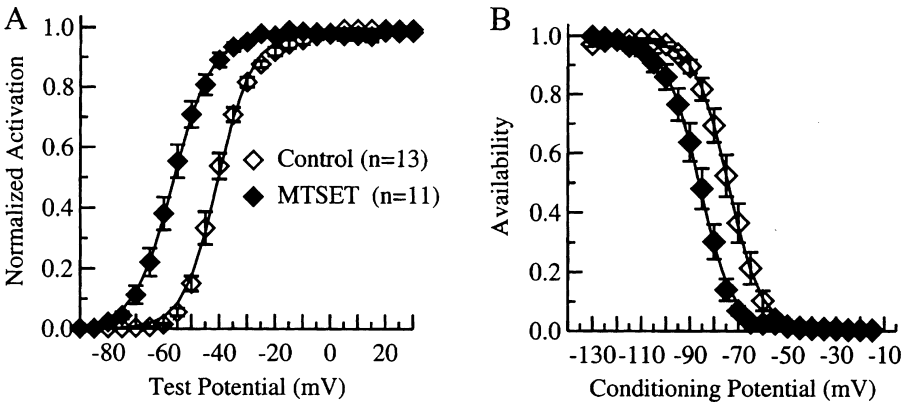

Fig. 7. Steady-state activation and inactivation during control and exposure to internal MTSET (3 mM) in cells expressing F1760C channels. (*A*) From a holding potential of −100 mV, 40 ms pulses were applied to various test potentials. The test potential was incremented in 5 mV steps. The activation-voltage relationship was fit to Boltzmann functions. Parameters for the fits are summarized in Table 2. (*B*) Na channel availability was determined by application of 500 ms conditioning pulses from −130 to −15 mV. A test pulse of −20 mV followed each conditioning pulse. Normalized test pulse currents were plotted against the conditioning voltage and fit to Boltzmann functions. Parameters for steady-state availability are summarized in Table 2.

block observed with the F1760C mutant, we performed the double mutant W374A/F1760C. Use-dependent block was not apparent with the double mutant at any holding potential (−120, −100, and −90 mV) or cycle length (150 – 1500 ms). For example, the mean value of the normalized peak current of the 40th pulse was 1.03 ± 0.02 (n = 7) that of the first-pulse current for trains of cycle length of 150 ms applied from a holding potential of −90 mV.

Gating Characteristics in the Presence of Drug

We assessed the gating characteristics of F1760A and F1760C mutant sodium channels in the presence of lidocaine and MTS-ET. In our experiments the F1760A hH1 mutant exhibited no sensitivity to 800 μM lidocaine. We assessed the level of use-dependent block of the FC mutant in the presence of 800 μM lidocaine. Current reduction during repetitive stimulation beyond that which was observed at baseline would indicate sensitivity to lidocaine. Pulse-train stimulation was performed as described above. The use-dependent current reduction in the presence of lidocaine was increased over that of the FC mutant at baseline for all cycle lengths and holding potentials. Although this fractional current reduction was greater, it was significantly less than the use-dependent block exhibited by WT channels exposed to lidocaine. Use-dependent block was enhanced at depolarized holding potentials. Summary data for the response of hH1, F1760A, and F1760C are presented in Fig. 6.

So far we have shown that the FC mutant sodium channel exhibits baseline use-dependent current reduction and altered gating, likely as the result of a larger component of slow inactivation. We have also shown that, unlike the FA mutant channels, FC channels display sensitivity to lidocaine, although reduced when compared to WT channels. We next assessed behavior of the wild-type and FC channels with modification by MTS-ET. MTS-ET was without effect on the wild-type channel (summarized in Fig. 5). MTS-ET should bind to the cysteine substituent covalently and not dissociate from the channel. If use-dependent current reduction involves alternate association and dissociation of drug from the receptor, then covalent modification of the substituted cysteine should lead to progressive current reduction with little rest recovery.

First, we examined the effects of internal MTS-ET on the equilibrium parameters of fast gating. Figure 7 illustrates the effects of MTS-ET on the activation and inactivation–voltage relationship. MTS-ET produced a 15 mV negative shift in $V_{1/2m}$ compared with control. $V_{1/2h}$ was also shifted by −15 mV. In the presence of MTS-ET, $V_{1/2m}$, $V_{1/2h}$ and the slope factors k_m and k_h were not different from those of hH1. In addition to these gating effects, MTS-ET significantly reduced the peak sodium current in cells expressing the FC mutation (−5.4 ± 0.5 vs −2.3 ± 0.3nA).

The negative shift in $V_{1/2h}$ could contribute to a reduction of sodium current during pulse train stimulation. As illustrated in Fig. 8*A*, MTS-ET enhanced the use-dependent reduction of sodium current using trains of 40 ms pulses at an interpulse interval of 150 ms. The enhanced current reduction showed rest recovery, despite the postulated covalent binding of MTS-ET to cysteine. Recovery during control and MTS-ET exposure was best fit by the sum of two exponentials. The fast time constant was significantly prolonged in the presence of MTS-ET. However, the slow time constants were the same. The extent of slow inactivation was enhanced by MTSET. Summary data are presented in Fig. 8*B* and *C* and Table 2.

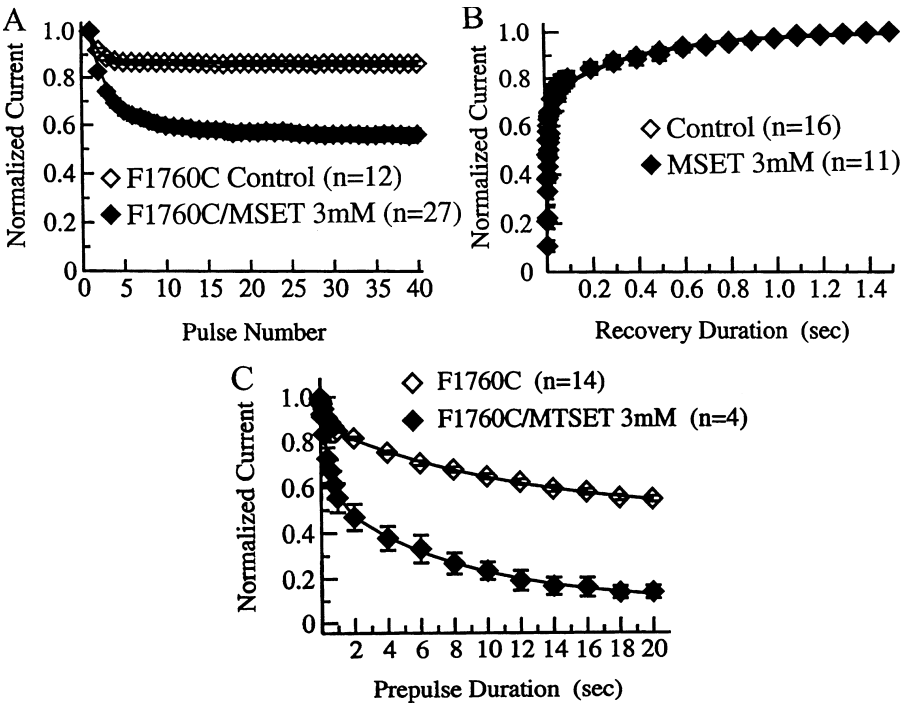

Fig. 8. Membrane current kinetics in cells expressing F1760C channels during control and intracellular exposure to 3 mM MTSET. (*A*) Normalized current during the application of trains of forty 40 ms pulses from a holding potential of −100 mV to a test potential of −20 mV. The interpulse interval was 150 ms. Control and MTSET experiments were performed in separate cells. (*B*) Kinetics of recovery from slow inactivation. From a holding potential of −100 mV, a 10-s conditioning pulse was applied to +60 mV; after a variable recovery interval, a test pulse was applied to −20 mV. Normalized test pulse current is plotted against recovery interval. (*C*) Measurement of the kinetics of development of slow inactivation. From a holding potential of −100 mV, a conditioning voltage step of increasing duration was applied to +60 mV. Return to −100 mV for 200 ms permitted recovery from fast inactivation. A test pulse to −20 mV assessed the residual slow inactivation.

Table 3. Parameters of slow gating kinetics

	hH1	F1760C	F1760C/MTSET
Steady-state slow inactivation			
$V_{1/2}$, mV (n)*	−63.3 ± 4.5 (7)	−41.7 ± 3.0 (6)	
K	42.8 ± 2.1	25.5 ± 1.8	
Onset of slow inactivation			
τo, s (*n*)	6.01 ± 0.59 (3)	4.61 ± 0.18 (14)	1.37 ± 0.25 (4)
Recovery from slow inactivation			
τr, s (*n*)	0.078 ± 0.005 (6)	0.270 ± 0.049 (4)	

Finally, we examined the influence of MTS-ET internally in combination with lidocaine externally. We wished to see whether lidocaine bound to its receptor site would protect the channel from MTS-ET effects. FC mutant cells were placed in a bath containing 800 μM of lidocaine. A pipette solution containing 3 mM of MTS-ET was used to obtain whole-cell currents during pulse-train stimulation. The level of use-dependent current reduction was determined and compared to that of the previous experiments. The level of use dependence paralleled that of the FC-ET mutant alone (Fig. 6*A*). Total block was not enhanced by the combined presence of lidocaine and MTS-ET.

Discussion

In the absence of drug exposure, the FC mutation resulted in use-dependent reduction of the sodium current at holding potentials of −90 and −100 mV. Sodium current recorded from cells expressing the FC mutant entered the slow inactivated state more rapidly and recovered more slowly. This observation suggests that the 1760 locus plays a role in the slow

inactivation process and links drug action to slow inactivation. The results also suggest dissociation between fast and slow inactivation. Some sequential models of inactivation propose that channels transition through a fast inactivated state before undergoing slow inactivation, while other models propose independent pathways to slow inactivation (Zilberter et al., 1991; Zilberter & Motin, 1991). Slow inactivation persists when fast inactivation is removed with the enzyme pronase or the oxidant chloramines-T (Wang & Wang, 1997; Rudy, 1978). Vedantham and Cannon (1998) showed that fast and slow inactivation are structurally distinct and not tightly coupled. The positive shift in $V_{1/2}$ $h\infty$ in the face of enhanced slow inactivation in the FC mutant would support the relative independence of the two processes.

The use-dependent reduction of sodium current during drug exposure is generally interpreted to indicate alternate drug association during depolarizing pulses and dissociation in the interval between pulses. An alternative or contributory mechanism envisions the slowing of one or more of the normal gating transitions of the Na channel during drug exposure. To test the latter idea, cells expressing the FC mutant Na channel were exposed to the sulfhydryl-modifying agent MTS-ET. Reactive cysteinyl residues undergo an electrophilic substitution reaction with thiosulfonates such as MTS-ET. This reaction is essentially irreversible (Brocklehurst, 1979). The covalent modification of the 1760C substituent may be associated with use-dependent sodium-current reduction, but complete recovery should not occur.

MTS-ET exposure enhanced the use-dependent sodium-current reduction at holding potentials of −90 and −100 mV. The observation that 800 μM lidocaine produces no further block during exposure of the FC mutant in the presence of MTS-ET suggests that lidocaine and MTS-ET are interacting with the same site. The rest-recovery from use-dependent block during exposure to MTS-ET suggests that use-dependence involves slow transitions of the channel without actual association and dissociation of drug from its receptor. The local anesthetic class drugs, such as lidocaine, which do not produce flickering open channel block, may reduce the sodium current by slowing gating transitions such as slow inactivation. Such a mechanism would be consistent with the recent studies by Lee & McKinnon (2004) showing that peptide gating blockers partition in the bilayer with a co-efficient of $\sim 10^4$ and influence motion of the gating paddle.

Multiple loci in the sodium-channel structure appear to play significant roles in slow inactivation. Metrovic et al. showed that the R1454C mutation in D1VS4 of hNa_v 1.4 displayed use dependence during exposure to MT-SES (Mitrovic, George & Horn, 2000). This action is antagonized by the W408A mutation in D1S5-S6 linker. Bendahhou et al. showed that the hyperkalemic periodic paralysis-associated mutation I1595F in the middle of DIVS5 enhances slow inactivation (Bendahhou et al., 1999).

The S5-S6 pore residues also play important roles in slow inactivation. Wang & Wang (1997) showed that a mutation of a conserved arginine to alanine in D1-S6 markedly enhanced slow inactivation. Kambouris et al., and Ong,. Tomaselli & Balser have demonstrated that mutations in the outer pore loops of domains 1 and III enhance slow inactivation; other mutations in the same region reduce lidocaine block (Kambouris et al., 1998) (Ong et al., 2000). Vilin et al. constructed chimeras of Na_v 1.4 and Na_v 1.5 and showed that the greater slow inactivation of Na_v 1.4 was transferrable with the S5-S6 pore loops (Vilin et al., 1999).

The effects of the F1760 A and C mutations on the cardiac sodium channel differ from that reported for the type III brain- and the skeletal muscle sodium channels. We observed a depolarizing shift in half potential for inactivation, similar to that reported by Ragsdale et al. (1994). However, Li et al. and Bai et al. observed a hyperpolarizing shift in the half potential for inactivation with the corresponding mutation (F1700C and F1579C) in the type III brain and skeletal muscle sodium channels, respectively (Li et al., 1999; Bai et al., 2003). This appears to be a genuine difference between the sodium-channel isoforms. Sunami et al. reported block of the mutant $Na_{1.4v}$, F1579C channel with both internal and external application of the thiosulfonate MTSEA. The external blocking action is clearly different from our observations with both charged and neutral thiosulfonates. With low rates of stimulation they observed an increase in sodium current with internal application of MTS-ET; we observed a decrease in sodium current only. Together, these observations emphasize the difference in the sodium-channel isoforms in their response to modification. (Sunami et al., 2004).

Khodorov, Shishkova, Peganov, and Revenko originally proposed that use-dependent block of the sodium current by local anesthetic class drugs resulted from the transition into a slow inactivated state (Khodorov et al., 1976). The transitions between the slow inactivated state can be modulated by $[K^+]o$, $[Ca^{2+}]o$, and pHo, factors that exert a significant effect on local anesthetic block. Local anesthetic drug action may be an extension of the intrinsic gating behavior of the channel. In our analysis, we considered a single slow inactivated state. However, the number of identifiable slow inactivated states increases as the upper time limit of voltage-clamp protocols is extended.

References

Bai, C.-X., Glaaser, I.W., Sawanobori, T., Sunami, A. 2003. Involvement of local anesthetic binding sites on IVS6 of sodium channels in fast and slow inactivation. *Neurosci. Lett.* **337:**41–45

Bean, B.P., Shrager, P., Goldstein, D.A. 1981. Modification of sodium and potassium channel gating kinetics by ether and halothane. *J. Gen. Physiol.* **77:**233–253

Bendahhou, S., Cummins, T.R., Tawil, R., Waxman, S.G., Ptacek, L.J. 1999. Activation and inactivation of the voltage-gated sodium channel: Role of segment S5 revealed by a novel hyperkalaemic periodic paralysis mutation. *J. Neuroscience* **19:**4762–4771

Brocklehurst, K. 1979. Specific covalent modification of thiols: Applications in the study of enzymes and other biomolecules. *Int. J. Biochem.* **10:**259–274

Gilliam, F.R.I., Starmer, C.F., Grant, A.O. 1989. Blockade of rabbit atrial sodium channels by lidocaine: Characterization of continuous and frequency-dependent blocking. *Circ. Res.* **65:**723–739

Grant, A.O., Chandra, R., Keller, C., Carboni, M., Starmer, C.F. 2000. Block of wild-type and inactivation-deficient cardiac sodium channels IFM/QQQ stably expressed in mammalian cells. *Biophys. J.* **79:**3019–3035

Grant, A.O., Wendt, D.J., Zilberter Y., Starmer, C.F. 1993. Kinetics of interaction of disopyramide with the cardiac sodium channel: Fast dissociation from open channels at normal rest potentials. *J. Membrane Biol.* **136:**199–214

Hondeghem, L.M., Katzung, B.G. 1977. Time- and voltage-dependent interactions of antiarrhythmic drugs with cardiac sodium channels. *Biochim. Biophys. Acta.* **472:**373–398

Kambouris, N.G., Hastings, L.A., Stepanovic, S., Marban, E., Tomaselli, G.F., Basler, J.R. 1998. Mechanistic link between lidocaine block and inactivation probed by outer pore mutations in the rat μ1 skeletal muscle sodium channel. *J. Physiol.* **512:**693–705

Khodorov, B., Shishkova, L., Peganov, E., Revenko, S. 1976. Inhibition of sodium currents in frog Ranvier node treated with local anesthetics. Role of slow sodium inactivation. *Biochim. et Biophy. Acta* **433:**409–435

Kohlhardt M., Fichtner H., Froebe U. 1987. DPI-modified cardiac Na^+ channels open channel block by propafenone and pragmalium. Pfluegers Arch. 408:R 38

Lee, S.-Y., MaCKinnon, R. 2004. A membrane-access mechanism of ion channel inhibition by voltage sensor toxins from spider venom. *Nature* **430:**232–235

Li, H.-L., Galue, A., Meadows, L., Ragsdale, D.S. 1999. A molecular basis for the different local anesthetic affinities of resting versus open and inactivated states of the sodium channel. *Molec. Pharmacol.* **55:**134–141

Matsuki, N., Quandt, F.N., Ten Eick, R.E., Yeh, J.Z. 1984. Characterization of the block of sodium channels by phenytoin in mouse neuroblastoma Cells. *J. Pharamacol. Exp. Ther.* **228:**523–530

Mitrovoic, N., George Jr., A.L., Horn, R. 2000. Role of domain 4 in sodium channel slow inactivation. *J. Gen. Physiol.* **115:**707–717

Ong, B., Tomaselll, G., Basler, J. 2000. A structural rearrangement in the sodium channel pore linked to slow inactivation and use dependence. *J. Gen. Physiol.* **116:**653–661

Ragsdale, D.S., McPhee, J.C., Scheuer, T., Catteral, W.A. 1994. Molecular determinants of state-dependent block of Na^+ channels by local anesthetics. *Science* **265:**1724–1728

Rudy, B. 1978. Slow inactivation of the sodium conductance in squid giant axons. Pronase resistance. *J. Physiol.* **283:**1–21

Stricharytz, G.R. 1973. The inhibition of sodium currents in myelinated nerve by quaternary derivatives of lidocaine. *J. Gen. Physiol.* **62:**37–57

Sunami, A., Tracey, A., Glasser, I.W., Lipkind, M., Hanck, D.A., Fozzard, H.A. 2004. Accessibility of mid-segment domain IV S6 residues of the voltage-gated Na^+ channel to methanethiosulfonate reagents. *J. Physiol.* **561:**403–413

Vedantham, V., Cannon, S.C. 1998. Slow inactivation does not affect movement of the fast inactivation gate in voltage-gated Na^+ channels. *J. Gen. Physiol.* **111:**83–93

Vedantham, V., Cannon, S.C. 1999. The position of the fast-inactivation gate during lidocaine block of voltage-gated Na^+ channels. *J. Gen. Physiol.* **113:**7–16

Vilin, Y.Y., Makita, N., George Jr., A.L., Ruben, P.C. 1999. Structural determinants of slow inactivation in human cardiac and skeletal muscle sodium channels. *Biophys. J.* **77:** 1384–1393

Wang, S.-Y., Wang, G.K. 1997. A Mutation in segment I-S6 Alter slow inactivation of sodium channels. *Biophys. J.* **72:** 1633–1640

Zaborovskaya, L.D., Khodorov, B.I. 1984. The role of inactivation in the cumulative blockage of voltage-dependent sodium channels by local anesthetics and antiarrhythmics. *Gen. Physiol. Biophys.* **3:**517–520

Zhu, G., Zhang, Y., Xu, J., Hang, C. 1998. Identification of endogenous outward currents in the human embryonic kidney (HEK293) cell line. *J. Neuroci. Methods* **81:**73–83

Zilberter, Y., Motin, L., Sokolova, S., Papin., A., Khodorov, B. 1991. Ca-sensitive slow inactivation and lidocaine-induced block of sodium channels in rat cardiac cells. *J. Mol. Cell Cardiol.* **23:**Suppl 1, 61–72

Zilberter, Y.I., Motin, L.G. 1991. Existence of two fast inactivation states in cardiac Na channels confirmed by two-stage of proteolytic enzymes. *Biochim. Biophys. Acta.* **1068:**77–80